

Single-Inclusive Jet Production in Polarized pp Collisions at $\mathcal{O}(\alpha_s^3)$

B. Jäger^a, M. Stratmann^a, and W. Vogelsang^{b,c}

^a*Institut für Theoretische Physik, Universität Regensburg,
D-93040 Regensburg, Germany*

^b*Physics Department, Brookhaven National Laboratory,
Upton, New York 11973, U.S.A.*

^c*RIKEN-BNL Research Center, Bldg. 510a, Brookhaven National Laboratory,
Upton, New York 11973 – 5000, U.S.A.*

Abstract

We present a next-to-leading order QCD calculation for single-inclusive high- p_T jet production in longitudinally polarized pp collisions within the “small-cone” approximation. The fully analytical expressions obtained for the underlying partonic hard-scattering cross sections greatly facilitate the analysis of upcoming BNL-RHIC data on the double-spin asymmetry A_{LL}^{jet} for this process in terms of the unknown polarization of gluons in the nucleon. We simultaneously rederive the corresponding QCD corrections to unpolarized scattering and confirm the results existing in the literature. We also numerically compare to results obtained with Monte-Carlo methods and assess the range of validity of the “small-cone” approximation for the kinematics relevant at BNL-RHIC.

I Introduction

The first successful runs of the BNL-RHIC with polarized proton beams mark a new era in spin physics. Very inelastic pp collisions at high energies open up unique possibilities to answer many interesting questions, first and foremost perhaps those concerning the still unknown gluon polarization in the nucleon, Δg [1]. In the near-term this prime goal can be accomplished by studying double spin asymmetries A_{LL} for the inclusive production of hadrons and jets. Both are copiously produced at high energies, and luminosity requirements are rather modest for a first determination of Δg . Measurements of the unpolarized neutral pion cross section at a center-of-mass (c.m.s.) energy of $\sqrt{S} = 200$ GeV, for both central and forward pseudo-rapidities η by PHENIX [2] and STAR [3], respectively, have shown good agreement with perturbative QCD (pQCD) calculations, even down to unexpectedly small values of the pion transverse momentum p_T of about 1.5 GeV. This boosts confidence that similar measurements with polarized protons, too, may be interpreted in terms of pQCD. Very recently, PHENIX has published first results for A_{LL} in $pp \rightarrow \pi^0 X$ at moderate p_T , though preliminary and with rather limited statistics [4]. Surprisingly, the data show a trend towards a negative and sizable A_{LL} which, if it persists, would appear to be impossible to accommodate in the framework of leading twist pQCD [5]. More data are clearly needed before any definitive conclusions can be drawn. It is expected that STAR will soon publish data on the spin asymmetry A_{LL}^{jet} for the closely related jet production. It will be particularly interesting to see whether these data will show a similar trend as the PHENIX π^0 data. This paper presents new theoretical pQCD calculations and predictions for the spin asymmetry in jet production, which appears timely in view of the experimental situation.

In order to make reliable quantitative predictions and to analyze upcoming data in terms of spin-dependent parton densities it is crucial to know the next-to-leading order (NLO) QCD corrections to the lowest order (LO) Born approximation for the partonic hard-scatterings. NLO corrections can be sizable and may affect the spin asymmetries. More importantly, the dependence on unphysical factorization and renormalization scales is expected to be reduced by the inclusion of higher order corrections. In case of jet production, NLO corrections are also of particular importance since it is only at NLO that the QCD structure of the jet starts to play a role in the theoretical description, providing for the first time the possibility and necessity to match the experimental conditions imposed to group final-state partons into a jet.

The past few years have seen much progress in calculations of NLO QCD corrections to spin-dependent processes relevant for the RHIC spin program. In particular for inclusive hadron production, NLO results have been obtained recently both at an analytical level [6] as well as using Monte-Carlo integration techniques [7]. While the latter basically allow to compute

any infrared-safe cross section numerically, the former is restricted to inclusive hadron spectra. However, fully analytical calculations lead to much faster and more efficient computer codes as all singularities arising in intermediate steps have explicitly canceled and are not subject to delicate numerical treatments. Such calculations will greatly facilitate a future “global analysis” of RHIC data in terms of polarized parton densities, e.g., along the lines described in [8].

The aim of this paper is to obtain (approximate) *analytical* NLO QCD results also in the case of single-inclusive high- p_T jet production in longitudinally polarized pp collisions. NLO corrections to polarized jet production have been determined before, using Monte-Carlo methods [9]. However, for the reason just given, we believe that our calculation is a very useful addition and of great relevance in practice. Its results will be immediately usable in a phenomenological analysis of forthcoming STAR data.

The actual calculation of the partonic cross sections up to NLO is a formidable task. Fortunately, inclusive hadron and jet production proceed through the same set of partonic subprocesses, and it turns out that we can make use of much of what we already calculated previously in the case of hadron production [6]. The main difference is in the treatment of final-state singularities: in case of inclusive hadron production the phase space of all unobserved partons is fully integrated over. This leads to final-state singularities which are to be absorbed into the parton-to-hadron fragmentation functions. However, a jet is essentially defined as a transverse-energy deposition within a certain cone centered around pseudo-rapidity η^{jet} and azimuth ϕ^{jet} . For such an observable, all final-state singularities cancel [10]. As we will see below, despite this difference, it is possible to transform the single-parton-inclusive cross sections that we have calculated earlier [6] into single-inclusive jet cross sections. This can even be done at an analytical level if one assumes that the jet cone is rather narrow (“small-cone approximation”, SCA). This is the strategy we will use in this paper. We note that the SCA was first introduced many years ago [10, 11] and has been applied in computations of unpolarized single-inclusive jet cross sections [12]. We have re-done the calculations in the unpolarized case and fully confirm the results available in the literature [12]. By comparing our polarized cross sections obtained within the SCA to results of the NLO Monte-Carlo “parton generator” of [9] we can assess the range of applicability of the SCA. It turns out that for the kinematics relevant at RHIC the SCA is very accurate, and that our numerical code is orders of magnitude faster than the Monte-Carlo one. Thus our results will indeed be useful for the analysis of upcoming data in terms of polarized parton densities.

The outline of the paper is as follows: after defining our notation, the next section is mainly devoted to present in some detail the necessary technical framework to convert single-parton-

inclusive cross sections into jet cross sections. In Sec. III we present some phenomenological applications of our results, all tailored to upcoming measurements with the STAR experiment at the BNL-RHIC. First we compare the SCA to the Monte-Carlo results obtained for various cone sizes. Next we examine the size of the NLO corrections, the reduction of dependence on unphysical scales in NLO, and the sensitivity of the double-spin asymmetry A_{LL} to Δg . We summarize the main results in Sec. IV.

II Jet Production in the Small-Cone Approximation

II.1 Jet Definition and SCA

We will consider the single-inclusive jet cross section for the reaction $pp \rightarrow \text{jet } X$ which counts all events with a jet of a given transverse energy E_T^{jet} and pseudo-rapidity η^{jet} . Cross sections are infinite unless a finite jet “size” is imposed. Jets are not intrinsically well defined objects, but may be constructed in somewhat different fashions from a set of close-by final-state particles. In this work we define the jet four-momentum as the sum of the four-momenta of all particles inside a geometrical cone of half-aperture δ around the jet axis, given by the three-momentum of the jet, see Fig. 1. We treat the jet in the SCA [11, 12] as this allows for a largely analytical calculation of the cross section.

Other jet definitions and algorithms are clearly possible and, in fact, more widely used in practice [13-17]. A popular choice [14], also adopted in the jet analyses at STAR, is to define a jet as a deposition of total transverse energy $\sum_i E_T^i$ of all final-state particles that fulfill

$$(\eta^{\text{jet}} - \eta^i)^2 + (\phi^{\text{jet}} - \phi^i)^2 \leq R^2 . \quad (1)$$

Here η^i and ϕ^i denote the pseudo-rapidities and azimuthal angles of the particles, and R is the jet cone aperture. The jet variables are defined by $E_T^{\text{jet}} = \sum_i E_T^i$, $\eta^{\text{jet}} = -\ln[\tan(\theta^{\text{jet}}/2)] = \sum_i E_T^i \eta^i / E_T^{\text{jet}}$, and $\phi^{\text{jet}} = \sum_i E_T^i \phi^i / E_T^{\text{jet}}$. It has been shown [18] that in the SCA the jet definition we have adopted becomes equivalent to that given by Eq. (1), provided δ is chosen as $R/\cosh(\eta^{\text{jet}})$. We have verified this equivalence numerically using the Monte-Carlo code of [9]. Differences arise only at $\mathcal{O}(\delta^2)$ and are negligible for small cone apertures.

The SCA may be viewed as an expansion of the partonic cross sections around $\delta = 0$ (or, equivalently, $R = 0$). For small δ , the dependence on the cone size is of the form $\mathcal{A} \log(\delta) + \mathcal{B} + \mathcal{O}(\delta^2)$. In this work we determine the coefficients \mathcal{A} and \mathcal{B} at an analytical level. We neglect the $\mathcal{O}(\delta^2)$ pieces; we will demonstrate in Sec. III that this is a surprisingly good approximation

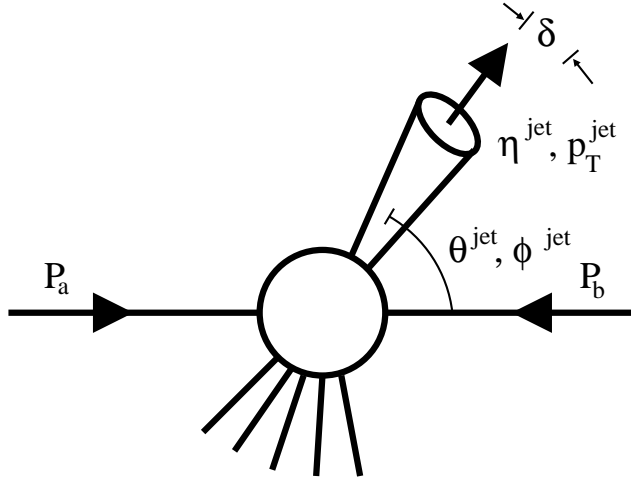


Figure 1: Sketch of single-inclusive jet production in $p(P_a)p(P_b) \rightarrow \text{jet}(P_{\text{jet}}) X$.

even for (experimentally relevant) cone sizes of up to $R \simeq 0.7$. This observation was also made some time ago for unpolarized jet cross sections by comparing the SCA to a calculation where the SCA was extended numerically to finite cone sizes [19, 20].

II.2 Notation and Outline of the Calculation

According to the factorization theorem for high- p_T processes [21], the spin-dependent cross section for single-inclusive jet production $p(P_a)p(P_b) \rightarrow \text{jet}(P_{\text{jet}}) X$ can be written as

$$\begin{aligned}
 \frac{d\Delta\sigma}{dp_T^{\text{jet}} d\eta^{\text{jet}}} &= \frac{1}{2} \left[\frac{d\sigma^{++}}{dp_T^{\text{jet}} d\eta^{\text{jet}}} - \frac{d\sigma^{+-}}{dp_T^{\text{jet}} d\eta^{\text{jet}}} \right] \\
 &= \frac{2p_T^{\text{jet}}}{S} \sum_{a,b} \int_{VW}^V \frac{dv}{v(1-v)} \int_{VW/v}^1 \frac{dw}{w} \Delta f_a(x_a, \mu_F) \Delta f_b(x_b, \mu_F) \\
 &\quad \times \left[\frac{d\Delta\hat{\sigma}_{ab \rightarrow \text{jet}X}^{(0)}(s, v)}{dv} \delta(1-w) + \frac{\alpha_s(\mu_R)}{\pi} \frac{d\Delta\hat{\sigma}_{ab \rightarrow \text{jet}X}^{(1)}(s, v, w, \mu_F, \mu_R; \delta)}{dvdw} \right], \quad (2)
 \end{aligned}$$

where the superscripts in Eq. (2) denote the helicities of the colliding polarized protons. The sum in Eq. (3) is over all contributing partonic channels $a + b \rightarrow \text{jet} + X$, with their associated LO and NLO partonic cross sections $d\Delta\hat{\sigma}_{ab \rightarrow \text{jet}X}^{(0)}$ and $d\Delta\hat{\sigma}_{ab \rightarrow \text{jet}X}^{(1)}$, respectively. The latter are defined in complete analogy with Eq. (2), the helicities now referring to partonic ones. In Eq. (3) we have introduced the dimensionless variables V and W which are defined in terms of p_T^{jet} and η^{jet} as

$$V = 1 - \frac{p_T^{\text{jet}}}{\sqrt{S}} e^{\eta^{\text{jet}}} \quad \text{and} \quad W = \frac{(p_T^{\text{jet}})^2}{SV(1-V)}, \quad (4)$$

with $S = (P_a + P_b)^2$ the available hadronic c.m.s. energy squared. The corresponding parton-level variables read

$$v \equiv 1 + \frac{t}{s} \quad , \quad w \equiv \frac{-u}{s+t} \quad , \quad s \equiv (p_a + p_b)^2 \quad , \quad t \equiv (p_a - P_{\text{jet}})^2 \quad , \quad u \equiv (p_b - P_{\text{jet}})^2 \quad , \quad (5)$$

where P_{jet} is the four-momentum of the jet ($P_{\text{jet}}^2 \simeq 0$ in the SCA). The information on the spin structure of the proton in Eq. (3) is contained in the spin-dependent parton densities $\Delta f_{a,b}$. They are probed at momentum fractions $x_{a,b}$ given by

$$x_a = \frac{VW}{vw} \quad \text{and} \quad x_b = \frac{1-V}{1-v} \quad . \quad (6)$$

The factorized structure of Eq. (3) dictates the appearance of the factorization scale μ_F which is of the order of the hard scale in the reaction, p_T^{jet} , but not further specified. The same is true for the scale μ_R associated with the renormalization of the running strong coupling $\alpha_s(\mu_R)$. Compared to single-inclusive hadron production [6, 7] the jet observables in Eq. (3) have the advantage of being free of uncertainties associated with the factorization of final-state singularities into non-perturbative parton-to-hadron fragmentation functions at a scale μ'_F . Hence, jet production at RHIC is expected to provide particularly clean and useful information on the spin structure of the proton.

As indicated above, the jet cross sections at the parton-level may be evaluated in pQCD as an expansion in the strong coupling α_s ,

$$d\Delta\hat{\sigma}_{ab \rightarrow \text{jet}X} = d\Delta\hat{\sigma}_{ab \rightarrow \text{jet}X}^{(0)} + \frac{\alpha_s}{\pi} d\Delta\hat{\sigma}_{ab \rightarrow \text{jet}X}^{(1)} + \dots \quad . \quad (7)$$

The LO approximation of Eq. (7), $d\Delta\hat{\sigma}_{ab \rightarrow \text{jet}X}^{(0)}$, is obtained from evaluating all basic $2 \rightarrow 2$ QCD scattering diagrams, that is, X consists of only one parton recoiling from the other parton producing the observed jet. Contrary to single-inclusive hadron production where different final-state partons have to be weighted with different fragmentation functions leading to ten separate LO channels [6], for a jet cross section no distinction is made between different quark flavors or gluons producing the jet. All processes with the same initial-state partons have to be summed appropriately, which is precisely the reason why final-state singularities cancel at higher orders. One then has only six different subprocesses :

$$\begin{aligned} qq' &\rightarrow \text{jet } X \\ q\bar{q}' &\rightarrow \text{jet } X \\ qq &\rightarrow \text{jet } X \\ q\bar{q} &\rightarrow \text{jet } X \\ qg &\rightarrow \text{jet } X \\ gg &\rightarrow \text{jet } X \quad . \end{aligned} \quad (8)$$

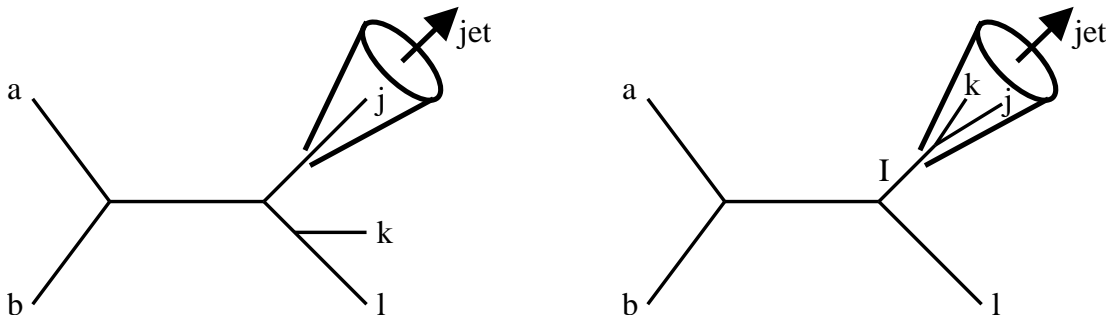


Figure 2: Contributions to the single-inclusive jet cross section from partonic reactions where only one parton is in the cone (left hand side) and where two essentially collinear partons, j and k , form a narrow jet (right hand side).

For the computation of the NLO corrections to Eq. (7), $d\Delta\hat{\sigma}_{ab\rightarrow\text{jet}X}^{(1)}$, we would like to make use as much as possible of the single-parton-inclusive cross sections that we have calculated earlier [6]. In the following we will demonstrate how to convert *analytically* the single-parton-inclusive cross sections into jet cross sections. In order to achieve this, we use the SCA and that the jet is formed either by a single final-state parton or by two partons essentially collinear to each other, see Fig. 2.

The connection between the two types of inclusive partonic cross sections can be best understood in the following way [11, 20]: let us consider the generic $2 \rightarrow 3$ partonic reaction $a(p_a) b(p_b) \rightarrow j(p_j) k(p_k) l(p_l)$. Partons a and b are longitudinally polarized here, which is however not really of any relevance in what follows. In [6] we have already computed at an analytical level the single-parton inclusive cross sections for $ab \rightarrow jX$, $ab \rightarrow kX$, and $ab \rightarrow lX$. Each one of these already contains a full sum over unobserved partonic final states X , that is, $ab \rightarrow jX$ would consist of $[ab \rightarrow j(k_1l_1)] + [ab \rightarrow j(k_2l_2)] + \dots$, in case several different final states are allowed. For instance, the channel $qg \rightarrow qX$ receives contributions from the partonic reactions $qg \rightarrow q(qg)$, $qg \rightarrow q(q\bar{q})$, $qg \rightarrow q(q'\bar{q}')$. With these stipulations, all three inclusive-parton processes, $ab \rightarrow jX$, $ab \rightarrow kX$, and $ab \rightarrow lX$, contribute also to single-inclusive jet production, for which they have to be added.

Looking closer at the cross section for $ab \rightarrow jX$ one has to distinguish configurations where only parton j is in the cone and forms the jet from situations where, for example, partons j and k (and similarly, j and l) are both in the cone, see Fig. 2. In the latter case, the single-parton-inclusive cross section still assumes that only parton j is observed, whereas for the jet cross section we want to define the jet from *both* partons inside the cone. We therefore subtract those parts from the single-parton-inclusive cross section for which j is observed, but k (or l) are in the cone. We proceed, of course, in the same way for the cross sections with k or l being

the observed parton. Finally, we have to *add* pieces for which j and k (or j and l , or k and l) are both in the cone, and for which j and k are forming the jet together. Note that these contributions are symmetric under exchange of j and k .

To be more specific, let us denote the longitudinally polarized single-parton-inclusive cross section for $ab \rightarrow jX$ by $d\Delta\hat{\sigma}_j$, the one where still j is observed, but k is also in the cone by $d\Delta\hat{\sigma}_{j(k)}$, and the one where j and k are in the cone and form the jet *together* by $d\Delta\hat{\sigma}_{jk}$. We then have the following final expression for the desired partonic jet cross section:

$$d\Delta\hat{\sigma}_{ab \rightarrow \text{jet}X} = [d\Delta\hat{\sigma}_j - d\Delta\hat{\sigma}_{j(k)} - d\Delta\hat{\sigma}_{j(l)}] + [d\Delta\hat{\sigma}_k - d\Delta\hat{\sigma}_{k(j)} - d\Delta\hat{\sigma}_{k(l)}] \\ + [d\Delta\hat{\sigma}_l - d\Delta\hat{\sigma}_{l(j)} - d\Delta\hat{\sigma}_{l(k)}] + d\Delta\hat{\sigma}_{jk} + d\Delta\hat{\sigma}_{jl} + d\Delta\hat{\sigma}_{kl} . \quad (9)$$

All final-state singularities of the individual cross sections are guaranteed to cancel in Eq. (9). Technically, because the $d\Delta\hat{\sigma}_j$ have already been made finite by an $\overline{\text{MS}}$ subtraction [6], we will first compute the combination

$$-d\Delta\hat{\sigma}_{j(k)} - d\Delta\hat{\sigma}_{j(l)} - d\Delta\hat{\sigma}_{k(j)} - d\Delta\hat{\sigma}_{k(l)} - d\Delta\hat{\sigma}_{l(j)} - d\Delta\hat{\sigma}_{l(k)} + d\Delta\hat{\sigma}_{jk} + d\Delta\hat{\sigma}_{jl} + d\Delta\hat{\sigma}_{kl} , \quad (10)$$

which will have final-state collinear singularities, the same (but with opposite sign) that were originally present in $d\Delta\hat{\sigma}_j + d\Delta\hat{\sigma}_k + d\Delta\hat{\sigma}_l$. To obtain a finite answer for the combination (10) an $\overline{\text{MS}}$ subtraction then has to be performed. A powerful check for the correct implementation of all contributions is to see that the dependence on the final-state factorization scale μ'_F present in the intermediate results disappears identically for each of the subprocesses listed in Eq. (8) when $d\Delta\hat{\sigma}_j + d\Delta\hat{\sigma}_k + d\Delta\hat{\sigma}_l$, taken from [6], is finally combined with (10).

Clearly, the pieces $d\Delta\hat{\sigma}_{j(k)}$ and $d\Delta\hat{\sigma}_{jk}$ that we will subtract and add are dominated by configurations with two collinear final-state partons. These configurations produce the $\mathcal{A} \log(\delta) + \mathcal{B} + \mathcal{O}(\delta^2)$ behavior in δ mentioned earlier. For collinear kinematics, the calculation dramatically simplifies because the $2 \rightarrow 3$ matrix elements then factorize into $2 \rightarrow 2$ ones and LO splitting functions, allowing the calculation to be done largely analytically. The narrower one chooses the cone, the more dominant will the “collinear” terms become. This is the reasoning behind the use of the SCA.

We note that the separation in Eq. (9) in the context of the SCA was already considered in Refs. [11, 20] in the unpolarized case. In these references also some details of the calculations of the $d\hat{\sigma}_{j(k)}$ and $d\hat{\sigma}_{jk}$ were given. The aim of the following subsections is to make this paper self-contained by providing all essential calculational details, without however going to excessive length. In the next two subsections, we will address $d\Delta\hat{\sigma}_{j(k)}$ and $d\Delta\hat{\sigma}_{jk}$ separately.

II.3 Calculation of $d\Delta\hat{\sigma}_{j(k)}$

In this section we show how to calculate the ‘‘subtraction’’ contributions $d\Delta\hat{\sigma}_{j(k)}$ to Eq. (9) when parton j alone forms the jet but parton k is also in the cone. We note that this part of the calculation is very similar to what was done for the isolated prompt photon cross section [22], except for the fact that all possible parton-parton splittings will occur in our case. The leading contributions in the SCA result from a branching of an intermediate parton I (which could, of course, be of the same type as j and/or k), see Fig. 2. In the *collinear approximation*, the spin-dependent matrix element squared $\Delta|M|_{ab\rightarrow jkl}^2$ for the process $ab \rightarrow jkl$ factorizes into

$$\Delta|M|_{ab\rightarrow jkl}^2 \propto \frac{1}{2p_j \cdot p_k} \Delta|M|_{ab\rightarrow Il}^2 \left(s, v' = \frac{vw}{1-v+vw} \right) P_{jI}^<(z = 1 - v + vw) , \quad (11)$$

where all quantities are in $d = 4 - 2\varepsilon$ dimensions in order to regularize collinear singularities. The superscript ‘‘<’’ denotes that the d -dimensional $I \rightarrow j$ unpolarized splitting function $P_{jI}(z)$ is strictly at $z < 1$, that is, without its $\delta(1-z)$ contribution if $I = j$. $\Delta|M|_{ab\rightarrow Il}^2$ denotes the spin-dependent matrix element squared for the $2 \rightarrow 2$ process $ab \rightarrow Il$. In addition, we find

$$2p_j \cdot p_k = 2E_j^2 \frac{v(1-w)}{1-v+vw} (1 - \cos\theta_{jk}) , \quad (12)$$

with θ_{jk} the angle between partons j and k . The factor $1/(2p_j \cdot p_k)$ in (11) constitutes the only dependence on θ_{jk} in the collinear approximation. Integrating it over the $2 \rightarrow 3$ phase space gives

$$\begin{aligned} \int \frac{dPS_3}{dvdw} \frac{1}{(2p_j \cdot p_k)} &= \left[\frac{1}{8\pi} \left(\frac{4\pi}{s} \right)^\varepsilon \frac{1}{\Gamma(1-\varepsilon)} [v'(1-v')]^{-\varepsilon} \right] \frac{1}{8\pi^2} \left(\frac{4\pi}{s} \right)^\varepsilon \\ &\times \frac{1}{\Gamma(1-\varepsilon)} \frac{v}{1-v+vw} \left[\frac{E_j^2 v^2 (1-w)^2}{s} \right]^{-\varepsilon} \int_0^\delta d\theta_{jk} \frac{\sin^{1-2\varepsilon}\theta_{jk}}{1-\cos\theta_{jk}} , \end{aligned} \quad (13)$$

where δ is the cone opening, v' is as in Eq. (11), and the factor in square brackets in the first line is the usual $2 \rightarrow 2$ phase space in d dimensions. For small δ the angular integral in Eq. (13) is readily evaluated as

$$\int_0^\delta d\theta_{jk} \frac{\sin^{1-2\varepsilon}\theta_{jk}}{1-\cos\theta_{jk}} = -\frac{\delta^{-2\varepsilon}}{\varepsilon} + \mathcal{O}(\delta^2) . \quad (14)$$

For the d -dimensional partonic cross section at $\mathcal{O}(\alpha_s^3)$ in the collinear approximation we then arrive at

$$\begin{aligned} \frac{d\Delta\hat{\sigma}_{ab\rightarrow jkl}}{dvdw} &= \frac{d\Delta\hat{\sigma}_{ab\rightarrow Il}}{dv} \left(v' = \frac{vw}{1-v+vw} \right) P_{jI}^<(z = 1 - v + vw) \\ &\times \frac{\alpha_s}{2\pi} \left(-\frac{1}{\varepsilon} \right) \frac{1}{\Gamma(1-\varepsilon)} \frac{v}{1-v+vw} \left[\frac{E_j^2 \delta^2 v^2 (1-w)^2}{s} \right]^{-\varepsilon} . \end{aligned} \quad (15)$$

Here, $d\Delta\hat{\sigma}_{ab\rightarrow Il}/dv$ denotes the d -dimensional Born cross section for $ab \rightarrow Il$. One can observe in Eq. (15) the expected separation into a universal part associated with the splitting function P_{jI} , and a part related to an underlying $2 \rightarrow 2$ partonic scattering.

From now on we will mainly focus on the splitting part, keeping in mind, however, that the appropriate sum over all partonic channels and splittings is implicitly understood in the end. The further evaluation is particularly simple when the splitting happens to be non-diagonal, i.e. $I \neq j$. In that case, the full splitting function P_{jI} is regular at $z = 1$, i.e., at $w = 1$, and all terms may be safely expanded in ε . The collinear singularity arising in Eq. (15) was also present in the single-parton-inclusive cross sections $d\Delta\hat{\sigma}_j$, where it was subtracted at a scale μ'_F into the bare parton-to-hadron fragmentation functions in the $\overline{\text{MS}}$ scheme [6]. This factorization is not appropriate for a jet cross section. In order to compensate for it, we have to apply the same subtraction also to Eq. (15). Any dependence on the factorization scale μ'_F will then drop out for the inclusive jet cross section in the sum (9) over partonic scatterings, as discussed above. The appropriate factorization term for Eq. (15) reads

$$\begin{aligned} \frac{d\Delta\hat{\sigma}_{\text{fact}}}{dvdw} &= -\frac{\alpha_s}{2\pi} \frac{d\Delta\hat{\sigma}_{ab\rightarrow Il}}{dv} \left(v' = \frac{vw}{1-v+vw} \right) P_{jI}^{(4)}(z = 1 - v + vw) \\ &\times \left(-\frac{1}{\varepsilon} \right) \frac{v}{1-v+vw} \left(\frac{\mu'_F{}^2}{s} \right)^{-\varepsilon}, \end{aligned} \quad (16)$$

where now $P_{jI}^{(4)}$ is the usual four-dimensional splitting function. Expressing the d -dimensional one as

$$P_{jI}(z) = P_{jI}^{(4)}(z) + \varepsilon P_{jI}^{(\varepsilon)}(z), \quad (17)$$

and adding Eqs. (15) and (16) we arrive at the final result for $d\Delta\hat{\sigma}_{j(k)}$ if $j \neq I$,

$$\begin{aligned} \frac{d\Delta\hat{\sigma}_{j(k)}}{dvdw} &= \frac{\alpha_s}{2\pi} \frac{v}{1-v+vw} \frac{d\Delta\hat{\sigma}_{ab\rightarrow Il}^{(d=4)}}{dv} \left(v' = \frac{vw}{1-v+vw} \right) \\ &\times \left[P_{jI}^{(4)}(z = 1 - v + vw) \ln \left(\frac{E_j^2 \delta^2 v^2 (1-w)^2}{\mu'_F{}^2} \right) - P_{jI}^{(\varepsilon)}(z = 1 - v + vw) \right], \end{aligned} \quad (18)$$

which is finite and shows the expected logarithmic dependence on δ .

For a diagonal splitting function in Eq. (15), i.e., $j = I$, the situation is somewhat more complicated due to the infrared singularity of $P_{jj}(z)$ at $z = 1$. The singularity is regularized by the factor $(1-w)^{-2\varepsilon}$ in (15) and gives rise to a $1/\varepsilon^2$ pole. This pole is then canceled by contributions from $d\Delta\hat{\sigma}_{jk}$, i.e., the cross section with both partons in the cone forming the jet. Rather than giving the lengthy (regularized) expression for the diagonal case, we therefore first turn to the calculation of $d\Delta\hat{\sigma}_{jk}$.

II.4 Calculation of $d\Delta\hat{\sigma}_{jk}$

Again, the leading configurations are those for which an outgoing intermediate parton I splits collinearly into two. We now have to deal with partons j and k in the cone producing the jet with four-momentum $P_{\text{jet}} = p_j + p_k$. Let us first note that for the d -dimensional $2 \rightarrow 3$ phase space one finds

$$\begin{aligned} 2E_{\text{jet}} \frac{dPS_3}{d^{d-1}P_{\text{jet}}} &= \frac{1}{(2\pi)^{5-4\varepsilon}} \int d^d p_j \delta(p_j^2) \frac{E_{\text{jet}}}{E_k} \delta([p_a + p_b - P_{\text{jet}}]^2) \\ &= \frac{1}{(2\pi)^{5-4\varepsilon}} \frac{1}{s\nu} \delta(1-w) \int d^d p_j \delta(p_j^2) \frac{E_{\text{jet}}}{E_k} . \end{aligned} \quad (19)$$

The cross sections $d\Delta\hat{\sigma}_{jk}$ thus contribute only at $w = 1$, i.e., with $2 \rightarrow 2$ kinematics. As discussed in the previous subsection the only dependence on θ_{jk} , the angle between the two partons j and k , stems from the propagator $\propto 1/(2p_j \cdot p_k)$. Integrating this term over the phase space (19) one finds after some algebra:

$$\begin{aligned} \int \frac{dPS_3}{d\nu dw} \frac{1}{(2p_j \cdot p_k)} &= \left[\frac{1}{8\pi} \left(\frac{4\pi}{s} \right)^\varepsilon \frac{1}{\Gamma(1-\varepsilon)} [v(1-v)]^{-\varepsilon} \right] \frac{1}{8\pi^2} \left(\frac{4\pi}{s} \right)^\varepsilon \delta(1-w) \\ &\quad \times \frac{1}{\Gamma(1-\varepsilon)} \int_0^{E_{\text{jet}}} dE_j \frac{E_{\text{jet}}}{E_k^2} \left(\frac{E_j^2}{s} \right)^{-\varepsilon} \int_0^{\theta_{\text{max}}} d\theta_j \frac{\sin^{1-2\varepsilon} \theta_j}{1 - \cos \theta_{jk}} , \end{aligned} \quad (20)$$

where θ_j is the angle of parton j with respect to the direction of the jet, \vec{P}_{jet} .

In order to find the relation between θ_j and θ_{jk} we first write

$$\cos \theta_{jk} = \frac{\vec{p}_j \cdot \vec{p}_k}{|\vec{p}_j| |\vec{p}_k|} = \frac{\vec{p}_j \cdot (\vec{P}_{\text{jet}} - \vec{p}_j)}{E_j (E_{\text{jet}} - E_j)} = \frac{|\vec{P}_{\text{jet}}| \cos \theta_j - E_j}{E_{\text{jet}} - E_j} \quad (21)$$

and then use

$$\vec{P}_{\text{jet}}^2 = (\vec{p}_j + \vec{p}_k)^2 = E_j^2 + (E_{\text{jet}} - E_j)^2 + 2E_j(E_{\text{jet}} - E_j) \cos \theta_{jk} . \quad (22)$$

Solving Eqs. (21) and (22) for θ_j , one finds in the collinear limit

$$\theta_j \approx \frac{E_{\text{jet}} - E_j}{E_{\text{jet}}} \theta_{jk} . \quad (23)$$

In the same way, one finds for the angle θ_k between parton k and the direction of the jet

$$\theta_k \approx \frac{E_j}{E_{\text{jet}}} \theta_{jk} . \quad (24)$$

It is important to keep in mind that neither of the two particles j and k is allowed to be outside the cone. In other words, the upper limit θ_{max} in Eq. (20) in terms of the cone opening δ is

$$\begin{aligned} E_k > E_j &: \quad \theta_{\text{max}} = \delta , \\ E_j > E_k &: \quad \theta_{\text{max}} = \frac{E_k}{E_j} \delta . \end{aligned} \quad (25)$$

We note that the integration over θ_j in Eq. (20) could also be written as an integration over the invariant mass $\sqrt{P_{\text{jet}}^2}$ of the jet. Consistently with the SCA, we have previously neglected the jet mass everywhere. However, the singularity of the cross section at $\theta_{jk} = 0$, where the jet mass vanishes, requires us to integrate over a finite region $0 \leq P_{\text{jet}}^2 \leq \mathcal{O}(\delta^2 E_{\text{jet}}^2)$ here.

We finally obtain, after performing the θ_j integration in Eq. (20) and introducing the variable $\xi = E_j/E_{\text{jet}}$,

$$\int \frac{dPS_3}{dvdw} \frac{1}{(2p_j \cdot p_k)} = \left[\frac{1}{8\pi} \left(\frac{4\pi}{s} \right)^\varepsilon \frac{1}{\Gamma(1-\varepsilon)} [v(1-v)]^{-\varepsilon} \right] \frac{1}{8\pi^2} \left(\frac{4\pi}{s} \right)^\varepsilon \delta(1-w) \\ \times \frac{1}{\Gamma(1-\varepsilon)} \left(-\frac{1}{\varepsilon} \right) \left(\frac{E_{\text{jet}}^2 \delta^2}{s} \right)^{-\varepsilon} \int_0^1 d\xi \left[\xi^{-2\varepsilon} \Theta\left(\frac{1}{2} - \xi\right) + (1-\xi)^{-2\varepsilon} \Theta\left(\xi - \frac{1}{2}\right) \right]. \quad (26)$$

Here, Θ denotes the Heaviside step-function, delineating the two regions specified in Eq. (25).

Eq. (11) obviously continues to hold. The difference between the calculation of $d\Delta\hat{\sigma}_{j(k)}$ in Sec. II.3 and of $d\Delta\hat{\sigma}_{jk}$ here is that we now need to integrate over the argument of the splitting function appearing in Eq. (11), as ξ in Eq. (26) plays the role of the momentum fraction z . To do so, let us denote

$$I_{mn} \equiv \int_0^1 d\xi \left[\xi^{-2\varepsilon} \Theta\left(\frac{1}{2} - \xi\right) + (1-\xi)^{-2\varepsilon} \Theta\left(\xi - \frac{1}{2}\right) \right] P_{mn}^<(\xi). \quad (27)$$

Then one straightforwardly computes the four relevant integrals I_{mn} :

$$I_{qq} = C_F \left[-\frac{1}{\varepsilon} - \frac{3}{2} + \varepsilon \left(-\frac{7}{2} + \frac{\pi^2}{3} - 3\ln(2) \right) \right] = I_{gq}, \\ I_{qg} = \frac{1}{2} \left[\frac{2}{3} + \varepsilon \left(\frac{23}{18} + \frac{4}{3}\ln(2) \right) \right], \\ I_{gg} = 2C_A \left[-\frac{1}{\varepsilon} - \frac{11}{6} + \varepsilon \left(-\frac{137}{36} + \frac{\pi^2}{3} - \frac{11}{3}\ln(2) \right) \right], \quad (28)$$

with $C_A = 3$ and $C_F = 4/3$ the usual SU(3) Casimir operators. Note that the $1/\varepsilon$ pole terms in Eqs. (28), along with the overall $1/\varepsilon$ singularity in Eq. (26), give double poles that exactly cancel the ones arising for collinear splittings in the $d\Delta\hat{\sigma}_{j(k)}$ (see the discussion at the end of Sec. II.3). This cancelation will be demonstrated in the next section. Furthermore, the term $-3/2$ in the first line of Eqs. (28) is identical to the negative of the coefficient of the $\delta(1-z)$ in the full P_{qq} splitting function. It is extremely important that we obtain this term: clearly, the factorization subtraction in Eq. (16) contains the *full* splitting function, whereas all collinear limits of $2 \rightarrow 3$ matrix elements, Eq. (11), give only the splitting functions *without* their $\delta(1-z)$ contributions. Without the term $-3/2$ above we would not be able to cancel the final-state singularities. The same happens if the intermediate parton I is a gluon: an outgoing gluon

may split into a gg or a $q\bar{q}$ pair, the latter coming in N_f “active” flavors. Again we find in Eqs. (28) the necessary $-11/6$ and $2/3$ factors, which combine to the LO QCD β -function, $\beta_0 = 11C_A/3 - 2N_f/3$, appearing in the $\delta(1-z)$ contribution to P_{gg} .

II.5 Collecting Results and Cancellation of Singularities

The rest of the calculation is essentially an exercise in bookkeeping of all of the many intermediate terms appearing in the various contributions to Eq. (9).

To be more specific, let us sketch an example: a process with a $q\bar{q}g$ final state. We already know $d\Delta\hat{\sigma}_q$, $d\Delta\hat{\sigma}_{\bar{q}}$, and $d\Delta\hat{\sigma}_g$ from the inclusive hadron calculation [6]. The pieces $d\Delta\hat{\sigma}_{g(q)}$ and $d\Delta\hat{\sigma}_{g(\bar{q})}$ rely on the splitting function P_{qq} and are treated by Eq. (18). Likewise, $d\Delta\hat{\sigma}_{q(\bar{q})}$ is related to P_{qq} . One only has to attach the appropriate LO cross section [depending on v' as defined above in Eq. (11)]. On the other hand, $d\Delta\hat{\sigma}_{q(g)}$ and $d\Delta\hat{\sigma}_{\bar{q}(g)}$ depend on the diagonal splitting function P_{qg} and are singular. It is therefore convenient to combine them directly with $d\Delta\hat{\sigma}_{qq}$ and $d\Delta\hat{\sigma}_{\bar{q}g}$, respectively. The combination $d\Delta\hat{\sigma}_{q(g)} - d\Delta\hat{\sigma}_{\bar{q}g}$ is, after $\overline{\text{MS}}$ subtraction of final-state collinear singularities at a scale μ'_F , proportional to

$$\begin{aligned}
d\Delta\hat{\sigma}_{q(g)} - d\Delta\hat{\sigma}_{\bar{q}g} &\propto \frac{\alpha_s}{2\pi} C_F \left\{ \delta(1-w) \left[\left(2 \ln v + \frac{3}{2} \right) \ln \left(\frac{\delta^2 E_{\text{jet}}^2}{\mu'^2_F} \right) + 2 \ln^2 v - \frac{7}{2} + \frac{\pi^2}{3} - 3 \ln(2) \right] \right. \\
&+ \frac{2}{(1-w)_+} \left[2 \ln v + \ln \left(\frac{\delta^2 E_{\text{jet}}^2}{\mu'^2_F} \right) \right] + 4 \left[\frac{\ln(1-w)}{1-w} \right]_+ \\
&\left. + \frac{v^2(1-w)}{1-v+vw} \left[1 + \ln \left(\frac{\delta^2 E_{\text{jet}}^2 v^2 (1-w)^2}{\mu'^2_F} \right) \right] \right\} . \tag{29}
\end{aligned}$$

This result is completely finite and may serve as a “building block” whenever there is an outgoing quark radiating a gluon. Only the appropriate longitudinally polarized LO cross section $d\Delta\hat{\sigma}_{ab\rightarrow ql}/dv$ has to be attached to Eq. (29), summed over all final-state partons l . The “+”-distribution in Eq. (29) is defined as usual by its integration with an appropriate test function:

$$\int_0^1 dw [g(w)]_+ f(w) = \int_0^1 dw g(w) [f(w) - f(1)] . \tag{30}$$

The final piece in this example is $d\Delta\hat{\sigma}_{q\bar{q}}$ which involves the integral I_{qg} in Eq. (28) and therefore is also singular. It is crucial here that we sum over *all* possible final state channels for two given colliding partons: if there is a contribution involving $d\Delta\hat{\sigma}_{q\bar{q}}$, there must also be one involving $d\Delta\hat{\sigma}_{gg}$. With the appropriate combinatorial prefactors these two will combine to a β_0 , as discussed above. Including also $d\Delta\hat{\sigma}_{g(g)}$, and after $\overline{\text{MS}}$ subtraction of final-state collinear

singularities, one obtains for the “building block” for intermediate gluons, i.e. $I = g$,

$$\begin{aligned}
& 2 d\Delta\hat{\sigma}_{g(g)} - 2N_f d\Delta\hat{\sigma}_{q\bar{q}} - d\Delta\hat{\sigma}_{gg} \\
& \propto \frac{\alpha_s}{2\pi} \left\{ \delta(1-w) \left[\left(2C_A \ln v + \frac{\beta_0}{2} \right) \ln \left(\frac{\delta^2 E_{\text{jet}}^2}{\mu_F'^2} \right) + C_A \left(2 \ln^2 v + \frac{\pi^2}{3} - \frac{17}{8} \right) \right. \right. \\
& \quad \left. \left. - \frac{11}{24}\beta_0 + \frac{1}{3}N_f - \beta_0 \ln(2) \right] + \frac{2C_A}{(1-w)_+} \left[2 \ln v + \ln \left(\frac{\delta^2 E_{\text{jet}}^2}{\mu_F'^2} \right) \right] + 4C_A \left[\frac{\ln(1-w)}{1-w} \right]_+ \right. \\
& \quad \left. + 2C_A \frac{v^2(1-w)}{(1-v+vw)^2} [1 + (1-v)^2 + vw(2-2v+vw)] \ln \left(\frac{\delta^2 E_{\text{jet}}^2 v^2(1-w)^2}{\mu_F'^2} \right) \right\}, \quad (31)
\end{aligned}$$

again finite. Recall that contributions from $d\Delta\hat{\sigma}_{q(\bar{q})}$, which also appear in Eq. (9), are associated with the non-diagonal splitting function P_{qg} and thus are finite by themselves and hence not included in (31). They are straightforwardly treated according to Eq. (18). Our main equations, Eqs. (18), (29), and (31), all show the expected “logarithmic plus constant”, i.e., $\mathcal{A} \log(\delta) + \mathcal{B} + \mathcal{O}(\delta^2)$, dependence on the jet cone opening δ . We note that the terms $\propto [\ln(1-w)/(1-w)]_+$ in Eqs. (29) and (31), which are the leading contributions at $w \rightarrow 1$, cancel identical pieces arising from the observed final-state parton in the single-parton inclusive cross sections $d\Delta\hat{\sigma}_q$, $d\Delta\hat{\sigma}_g$, so that such distributions are absent in the jet cross section. This finding is in accordance with results found in a large- w “threshold” resummation calculation of the jet cross section, when the jet is allowed to be massive at partonic threshold [23].

With these prerequisites at hand one can compute all relevant NLO partonic single-inclusive jet cross sections listed in Eq. (8) in the SCA. The final analytical results are too lengthy to be given here but can be found in a FORTRAN code which is available upon request from the authors. As mentioned already, a powerful check for the correctness of the calculation is the cancelation of any dependence on the final state factorization scale μ_F' when, according to Eq. (9), the single-parton-inclusive cross sections from [6] are combined with the appropriate combinations of $d\Delta\hat{\sigma}_{j(k)}$ and $d\Delta\hat{\sigma}_{jk}$ according to Eqs. (18), (29), and (31). All of our final results pass, of course, this consistency check. Another important check of the procedure outlined here comes from the computation of the unpolarized jet cross section in the SCA – the building blocks in Eqs. (29) and (31) have no memory of the polarization of the colliding partons which only enters through the LO $2 \rightarrow 2$ cross sections attached to them. We fully agree at an analytical level with the results of [12] which can be retrieved from their FORTRAN code, after an appropriate transformation to the $\overline{\text{MS}}$ factorization scheme.

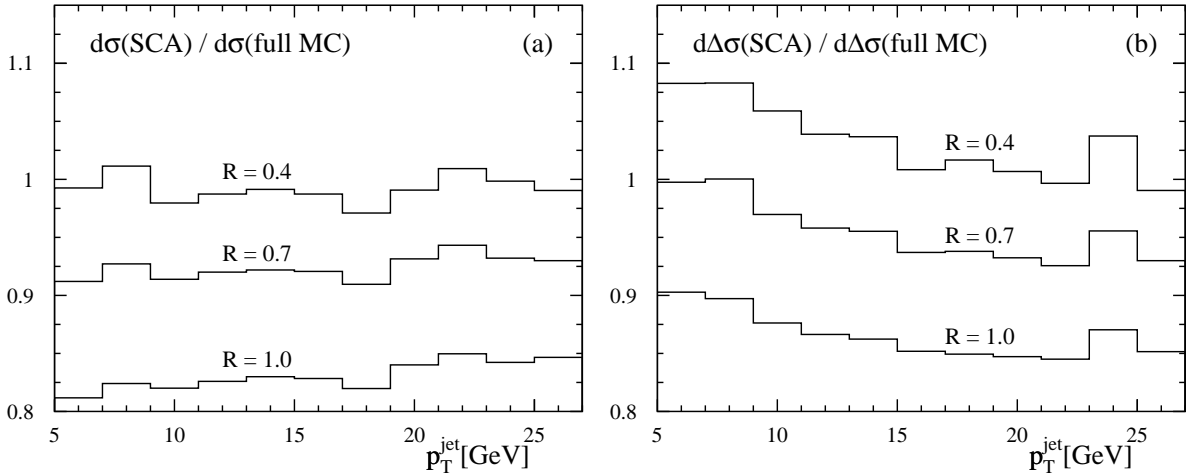


Figure 3: Ratio of the NLO (a) unpolarized and (b) polarized inclusive jet cross section in the SCA and within the full Monte-Carlo approach of [9] for $\sqrt{S} = 200$ GeV, several bins in p_T^{jet} , and three different cone sizes R .

III Numerical Results

We now turn to a phenomenological study of single-inclusive high- p_T jet production in polarized pp collisions at RHIC. Regarding our results obtained in the SCA, the most important question is, of course, how accurate the approximation actually is in cases of practical relevance. We will investigate this first, by comparing our results to those of the Monte-Carlo code of [9]. For this purpose, we choose the recent CTEQ6M set of unpolarized parton densities [24] in the calculation of the unpolarized cross section, and the NLO “standard” set of GRSV [25] for the polarized case. We assume the kinematical coverage of the STAR experiment, which can detect jets in the pseudo-rapidity range $-1 \leq \eta^{\text{jet}} \leq 1$, over which we integrate.

In Fig. 3 we compare the results of the full Monte-Carlo NLO jet calculation [9] to the results within the SCA for $\sqrt{S} = 200$ GeV, several bins in p_T^{jet} , and three different cone sizes R . The histograms on the left show the unpolarized results, the right ones give the comparison for the polarized case. It turns out that even for the rather large cone radius of $R = 0.7$ the SCA gives still very acceptable results within ten percent or less of the full Monte-Carlo calculation. For the unpolarized jet cross section such an observation was already made in [19, 20]. In the polarized case, however, the success of the SCA up to large R is non-trivial due to possible cancelations between the two helicity configurations in Eq. (2). Not unexpectedly, for very large $R = 1.0$ the SCA starts to break down because neglected contributions proportional to $\mathcal{O}(R^2)$ become relevant then. It is expected though that a cone size between 0.4 and 0.7 will be chosen by the STAR collaboration in their forthcoming analysis; larger sizes are not really

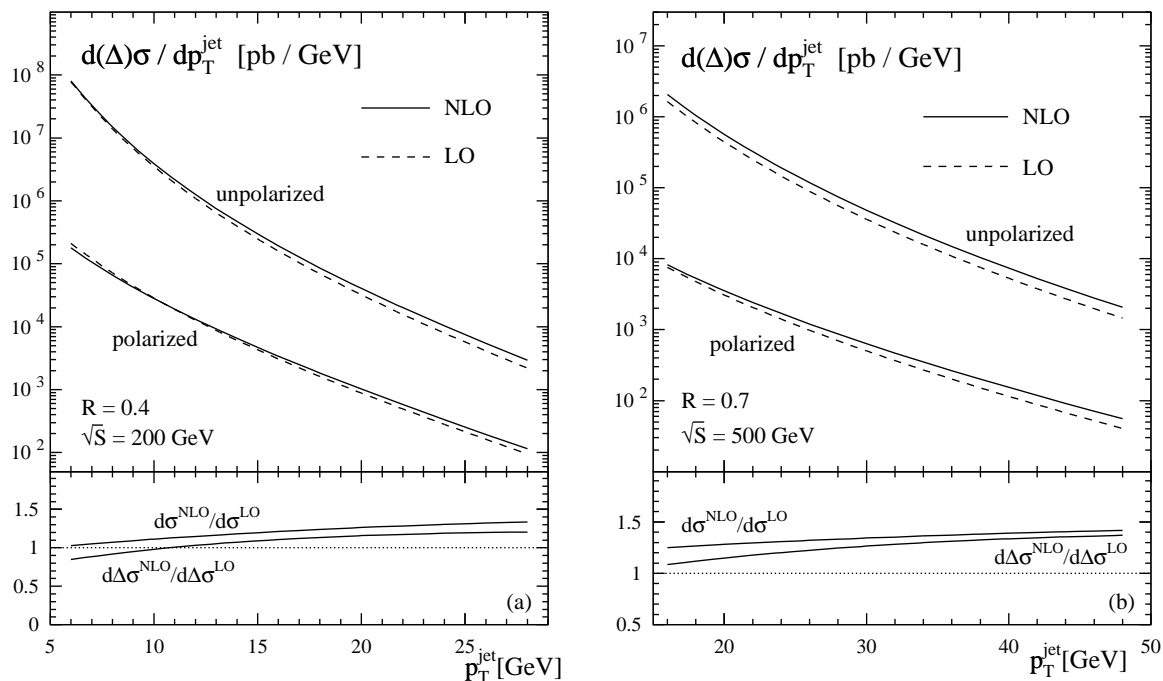


Figure 4: Unpolarized and polarized inclusive jet production cross sections in NLO (solid) and LO (dashed lines) at (a) $\sqrt{S} = 200$ GeV and (b) $\sqrt{S} = 500$ GeV for cone sizes $R = 0.4$ and $R = 0.7$, respectively. In each case the lower panel shows the ratios of the NLO and LO results.

practical in view of the limited angular acceptance of the detector.

Fig. 3 demonstrates that our results based on the SCA are sufficiently accurate to be used in analyses of forthcoming data on jet cross sections and spin asymmetries from RHIC. We emphasize that numerically stable results for the full p_T^{jet} spectrum can be obtained with our computer code very fast and efficiently, in a matter of minutes. This makes our code an ideal ingredient for future “global” analyses of RHIC jet data in terms of polarized parton densities. This is a clear advantage over a Monte-Carlo code with its huge numerical complexity, which yields results with rather large numerical fluctuations (still visible in the histograms shown in Fig. 3) even after hours of running. This is even more true for the polarized cross section due to large cancellations between the two helicity configurations in Eq. (2). That said, our present calculation can only be used to describe single-inclusive jet cross sections, whereas the Monte-Carlo code is much more flexible concerning the observables that can be predicted.

Heartened by the good agreement between our code and the full Monte-Carlo calculation, we will now present a few predictions for RHIC. We will be very brief here because many phenomenological results for jet production have already been presented in [9]. We focus on the most interesting questions: the importance of the NLO corrections, the residual dependence on the unphysical scales μ_F and μ_R in Eq. (3) at NLO, and the sensitivity of the double spin

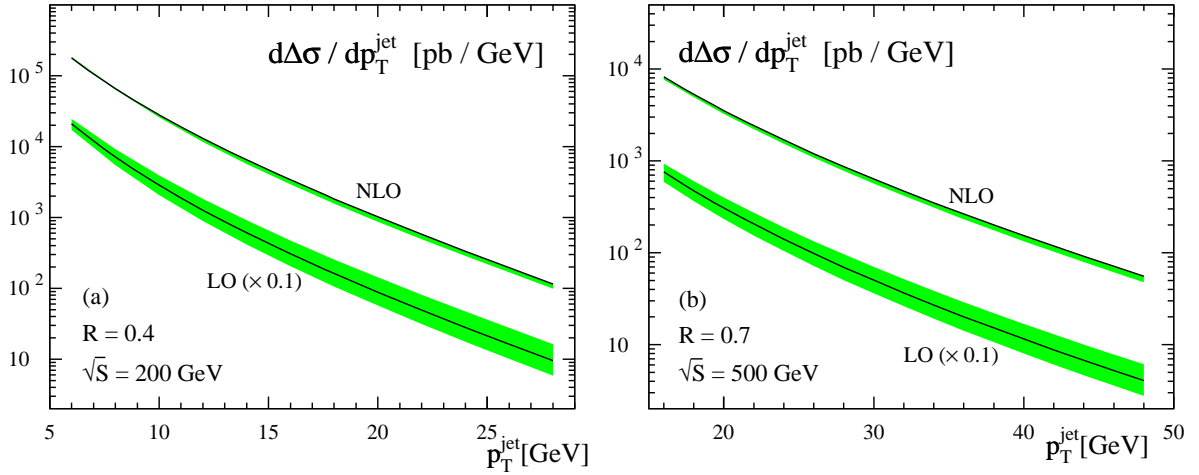


Figure 5: As in Figs. 4 (a) and (b) but now showing the scale dependence of the polarized cross section in LO and NLO in the range $p_T^{\text{jet}}/2 \leq \mu_F = \mu_R \leq 2p_T^{\text{jet}}$. We have rescaled the LO results by 0.1 to separate them better from the NLO ones. In each case the solid lines correspond to the choice where both scales are set to p_T^{jet} .

asymmetry

$$A_{\text{LL}}^{\text{jet}} \equiv \frac{d\Delta\sigma}{d\sigma} \quad (32)$$

to the still unknown gluon polarization Δg . Predictions for $A_{\text{LL}}^{\text{jet}}$ are in immediate demand for an extraction of Δg at RHIC in the very near future. In comparison to [9], there are also some new results in our analysis.

Figure 4 shows our results for the unpolarized and polarized p_T^{jet} -spectra of single-inclusive jets at NLO and LO, integrated over $-1 \leq \eta^{\text{jet}} \leq 1$, for $\sqrt{S} = 200$ GeV and $\sqrt{S} = 500$ GeV and cone sizes $R = 0.4$ and $R = 0.7$, respectively. We have set the scales $\mu_R = \mu_F = p_T^{\text{jet}}$. Again we have used CTEQ6M parton densities [24] in the unpolarized case and the GRSV “standard” set [25] for the polarized cross section, always performing the NLO (LO) calculations of cross sections using NLO (LO) sets of parton distribution functions and the two-loop (one-loop) expression for α_s . The lower part of the figure displays in each case the so-called “ K -factor”

$$K = \frac{d(\Delta)\sigma^{\text{NLO}}}{d(\Delta)\sigma^{\text{LO}}} \quad (33)$$

One can see that the NLO corrections are fairly moderate and of similar importance in the polarized and the unpolarized cases.

Figure 5 shows the scale dependence of the spin-dependent jet cross section at LO and NLO, again at $\sqrt{S} = 200$ GeV and $\sqrt{S} = 500$ GeV as in Figs. 4 (a) and (b), respectively. In each case the shaded bands indicate the uncertainties from varying the unphysical scales in the range

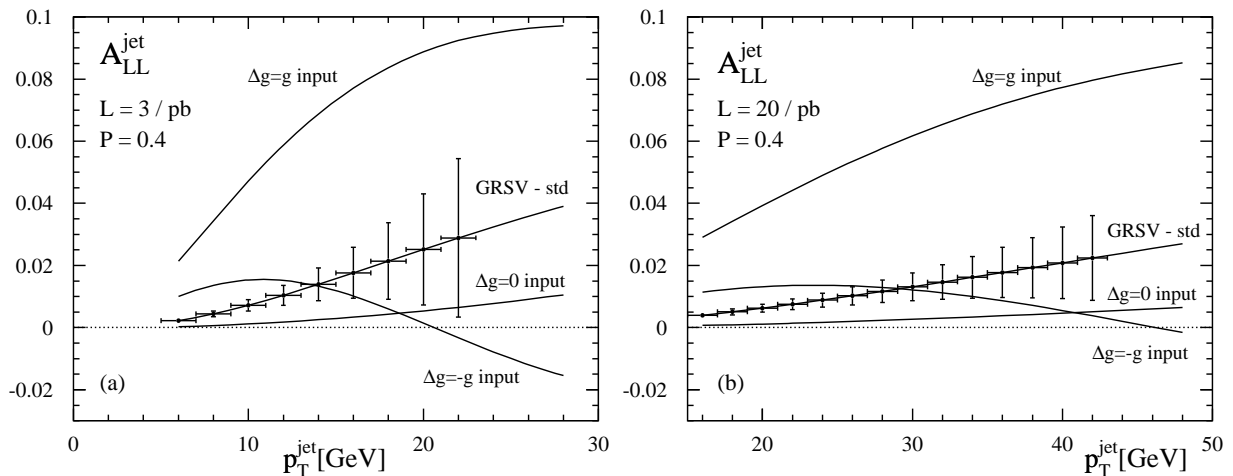


Figure 6: As in Figs. 4 (a) and (b) but now showing the spin asymmetry at NLO using the GRSV “standard” set [25] as well as three other sets with very different gluon polarizations (see text). The “error bars” indicate the expected statistical accuracy $\delta A_{LL}^{\text{jet}}$ for 40% beam polarization and integrated luminosities of 3 pb^{-1} and 20 pb^{-1} for $\sqrt{S} = 200 \text{ GeV}$ and $\sqrt{S} = 500 \text{ GeV}$, respectively (see text).

$p_T^{\text{jet}}/2 \leq \mu_R = \mu_F \leq 2p_T^{\text{jet}}$. The solid lines are for the choice where both scales are set to p_T^{jet} . Clearly, the scale dependence indeed becomes much smaller at NLO, a result that was already noted in [9]. We emphasize that the scale ambiguity of the single-inclusive jet cross section is somewhat smaller than for the corresponding single-inclusive hadron cross section, cf., Fig. 5 in [6]. This is not entirely unexpected, as the additional final-state factorization scale μ'_F related to the fragmentation of a parton into the observed hadron provides a further source of scale dependence not present for jet production.

Next we consider the double spin asymmetry A_{LL}^{jet} , Eq. (32), which is the main quantity of interest in experiment. Fig. 6 shows A_{LL}^{jet} , calculated at NLO for the “standard” set of GRSV parton densities [25], and for three other sets emerging from the GRSV analysis, which mainly differ in the assumptions about the gluon polarization: “ $\Delta g = g$ input”, “ $\Delta g = 0$ input”, and “ $\Delta g = -g$ input”. These are characterized by a large positive, a vanishing, and a large negative gluon polarization, respectively, at the input scale of the GRSV analysis [25]. We should note that all sets provide a good description of all presently available data on spin-dependent deep-inelastic scattering. Again we show results for both c.m.s. energies relevant for RHIC; the other parameters are chosen as before. Also shown is the expected statistical accuracy for such measurements in certain bins of p_T^{jet} for the STAR experiment, calculated from [1]

$$\delta A_{LL}^{\text{jet}} \simeq \frac{1}{\mathcal{P}_p^2 \sqrt{\mathcal{L}} \sigma_{\text{bin}}} . \quad (34)$$

We assume a moderate proton beam polarization \mathcal{P}_p of 40%. For the c.m.s. energy $\sqrt{S} =$

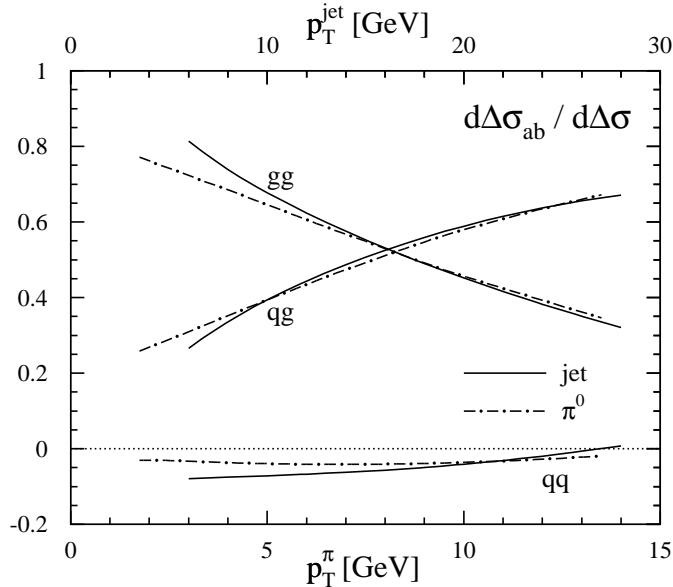


Figure 7: Relative contributions from gg , qg , and qq scatterings to the NLO polarized cross section for the “standard” set of GRSV [25] for jet and inclusive- π^0 production at mid pseudo-rapidities. Note that we use two separate coordinate axes for the two cases.

200 GeV we use an integrated luminosity \mathcal{L} of only 3 pb^{-1} which should be well accomplishable in the near-term future. Also, we assume that only half of the calorimeter is instrumented, i.e., we integrate only over $0 \leq \eta^{\text{jet}} \leq 1$. The error bars at $\sqrt{S} = 500 \text{ GeV}$ refer to $\mathcal{L} = 20 \text{ pb}^{-1}$ and $-1 \leq \eta^{\text{jet}} \leq 1$. Statistical accuracies for higher beam polarizations and/or luminosities are easily obtained by a proper rescaling of the error bars according to Eq. (34).

First and foremost we conclude from Figs. 6 that there are excellent overall prospects for determining Δg from A_{LL}^{jet} measurements at RHIC: the spin asymmetries for the different sets of polarized parton densities, which mainly differ in the gluon density, show marked differences, much larger than the expected statistical errors in the experiment even for the very moderate luminosities and beam polarizations assumed here. This finding was already highlighted in [9]. It is interesting, however, that at moderately small p_T^{jet} the spin asymmetry A_{LL}^{jet} is insensitive to the sign of Δg . A large negative gluon polarization yields an asymmetry somewhere in between the ones obtained with moderately and large positive gluon polarizations. This observation is very similar to the one recently made for inclusive hadron production at small transverse momentum [5]. It is due to the fact that at moderate p_T and mid pseudo-rapidities the gluon-gluon initiated subprocess is dominant. This process has a positive analyzing power and, since the two gluons are predominantly probed at very similar momentum fractions, it essentially probes the square of $\Delta g(x_a \simeq x_b)$. Thus a positive asymmetry is obtained even for a negative Δg . At larger jet transverse momenta, the qg process gradually takes over, resulting in sensitivity

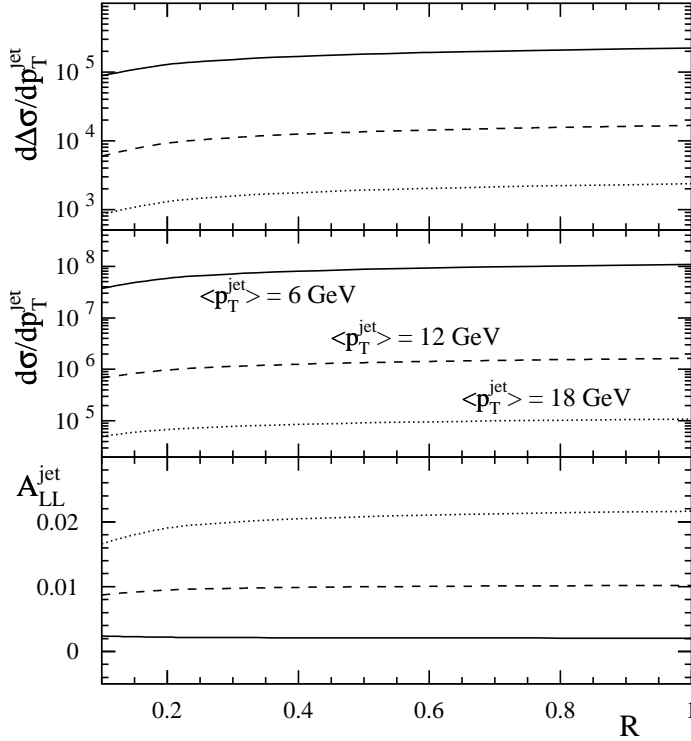


Figure 8: Cone radius R dependence of the polarized and unpolarized single-inclusive jet cross section and the corresponding spin asymmetry at NLO for $\sqrt{S} = 200$ GeV and three different p_T^{jet} bins. We have integrated over $-1 \leq \eta^{\text{jet}} \leq 1$.

of $A_{\text{LL}}^{\text{jet}}$ to the sign of $\Delta g(x_a \simeq x_b)$. When the c.m.s. energy is higher, the onset of the qg dominance occurs at higher p_T^{jet} since the spin asymmetry roughly scales with $x_T^{\text{jet}} = 2p_T^{\text{jet}}/\sqrt{S}$.

These properties of the partonic scatterings are exemplified by the solid lines in Fig. 7, which show the relative contributions to the polarized NLO cross section for the GRSV “standard” set for gg , qg , and qq scatterings at $\sqrt{S} = 200$ GeV. Here a “ q ” stands generically for the appropriate sum of all quark and anti-quark flavors. Each curve has been normalized to the full NLO cross section, so that the three lines add up to unity at every p_T^{jet} . For illustration, we also show in Fig. 7 the corresponding results for inclusive π^0 production [6] at mid pseudo-rapidities. We see that all curves for jets and pions are almost congruent, *provided* we rescale the axis for p_T^{π} by about a factor of 2. This feature is understood from the fact that pions result from a fragmentation process, in which the pion inherits only a certain momentum fraction z of a final-state parton. At RHIC energies, mid pseudo-rapidities, and for the transverse momenta we are considering here, one finds that the average z is about 0.5. This means that a pion of, say $p_T^{\pi} = 5$ GeV on average originates from a scattering in which a 10 GeV parton was produced. For the jet cross section, this parton would produce however a jet with $p_T^{\text{jet}} = 10$ GeV. This

explains the results in Fig. 7. Similar relations are also found for the spin asymmetries A_{LL}^{jet} and A_{LL}^{π} . This interesting predicted interplay between hadron and jet observables may be exploited to cross-check results and to gain a deeper insight into the dynamics producing high-transverse momentum final states.

We close by showing in Fig. 8 the dependence of the polarized and unpolarized single-inclusive jet cross sections and the corresponding spin asymmetry A_{LL}^{jet} on the cone size R in NLO QCD, for three representative bins in the jet's transverse momentum p_T^{jet} . We have chosen $\sqrt{S} = 200$ GeV and again integrated over pseudo-rapidity, $-1 \leq \eta^{\text{jet}} \leq 1$. The results for $\sqrt{S} = 500$ GeV are very similar and not shown here. We recall from Sec. II that for R not too large, the dependence on R is logarithmic. Obviously, at least in the unpolarized case, the cross section has to rise with increasing R . At larger R , deviations from our curves would be expected due to the terms $\propto R^2$ becoming important. A striking finding in Fig. 8 is that A_{LL}^{jet} turns out to depend only very mildly on R , in particular for p_T^{jet} not too large. We also note that since the cross section in Born approximation is independent of R , a measurement of the cone size dependence is a direct probe of NLO contributions.

IV Summary and Conclusions

In this paper we have presented a NLO calculation for the spin-dependent hadroproduction of single-inclusive jets. The application of the small cone approximation not only allowed us to perform the calculation at a largely analytical level but also to use major parts of a previous calculation for single-inclusive hadron production. We have outlined in some detail the connection between these two cross sections. By comparing to the Monte-Carlo jet code of [9] which treats the cone size exactly, we have demonstrated the applicability of the SCA up to cone sizes of about 0.7. Our code has the advantage of being numerically very stable and fast.

Our results are useful for studies of large- p_T jet production at RHIC, in particular for the analysis of upcoming data in terms of the unknown spin-dependent gluon density in the nucleon. We found that the NLO corrections to the (un)polarized cross section are well under control, and that their inclusion leads to a significant reduction of scale dependence, the main source of theoretical ambiguity. Even for rather moderate beam polarizations and integrated luminosities, the corresponding spin asymmetry shows a sensitivity to Δg . This makes single-inclusive jet production an excellent tool for fulfilling the short-term goal of RHIC: a first determination of the gluon polarization. Also in the long-run jet production data will provide invaluable information in a detailed mapping of the x -shape of spin-dependent parton densities.

The experimentally relevant spin asymmetry turned out to be rather insensitive to the precise definition of the jet as well as to the actual choice of the cone opening.

Acknowledgments

We are grateful to D. de Florian, E. Laenen, and G. Sterman for very valuable discussions and to J.-Ph. Guillet for providing us with matrix elements computed in [12]. B.J. and M.S. thank the RIKEN-BNL Research Center and Brookhaven National Laboratory for hospitality and support during different stages of this work and A. Schäfer for discussions. W.V. is grateful to RIKEN, Brookhaven National Laboratory and the U.S. Department of Energy (contract number DE-AC02-98CH10886) for providing the facilities essential for the completion of this work. This work was supported in part by the “Bundesministerium für Bildung und Forschung (BMBF)”.

References

- [1] See, for example: G. Bunce, N. Saito, J. Soffer, and W. Vogelsang, *Annu. Rev. Nucl. Part. Sci.* **50**, 525 (2000).
- [2] PHENIX Collaboration, S.S. Adler *et al.*, *Phys. Rev. Lett.* **91**, 241803 (2003).
- [3] STAR Collaboration, J. Adams *et al.*, [hep-ex/0310058](#) (to appear in *Phys. Rev. Lett.*).
- [4] A. Bazilevsky, talk presented at the “Xth Workshop on High Energy Spin Physics (Spin-03)”, Dubna, Russia, Sep. 16-20, 2003.
- [5] B. Jäger, M. Stratmann, S. Kretzer, and W. Vogelsang, *Phys. Rev. Lett.* **92**, 121803 (2004).
- [6] B. Jäger, A. Schäfer, M. Stratmann, and W. Vogelsang, *Phys. Rev.* **D67**, 054005 (2003).
- [7] D. de Florian, *Phys. Rev.* **D67**, 054004 (2003).
- [8] M. Stratmann and W. Vogelsang, *Phys. Rev.* **D64**, 114007 (2001).
- [9] D. de Florian, S. Frixione, A. Signer, and W. Vogelsang, *Nucl. Phys.* **B539**, 455 (1999).
- [10] G. Sterman and S. Weinberg, *Phys. Rev. Lett.* **39**, 1436 (1977).
- [11] M.A. Furman, *Nucl. Phys.* **B197**, 413 (1982).

- [12] F. Aversa, P. Chiappetta, M. Greco, and J.-Ph. Guillet, Nucl. Phys. **B327**, 105 (1989); Z. Phys. **C46**, 253 (1990).
- [13] S.D. Ellis, Z. Kunszt, and D.E. Soper, Phys. Rev. Lett. **62**, 726 (1989); Phys. Rev. **D40**, 2188 (1989); Phys. Rev. Lett. **64**, 2121 (1990).
- [14] John E. Huth *et al.*, published in the proceedings of the 1990 DPF “Summer Study on High Energy Physics: Research Directions for the Decade”, Snowmass, CO, USA, ed. E.L. Berger, World Scientific, 1992, p. 134.
- [15] UA2 Collaboration, J. Alitti *et al.*, Phys. Lett. **B257**, 232 (1991); CDF Collaboration, F. Abe *et al.*, Phys. Rev. **D45**, 1448 (1992); D0 Collaboration, S. Abachi *et al.* Phys. Rev. **D53**, 6000 (1996).
- [16] S. Catani, Yu.L. Dokshitzer, M.H. Seymour, and B.R. Webber, Nucl. Phys. **B406**, 187 (1993); S.D. Ellis and D.E. Soper, Phys. Rev. **D48** (1993) 3160.
- [17] See also the discussions about jet definitions and algorithms in, e.g.: W.B. Kilgore and W.T. Giele, Phys. Rev. **D55**, 7183 (1997); M.H. Seymour, Nucl. Phys. **B513**, 269 (1998); proceedings of the “8th International Workshop on Deep Inelastic Scattering and QCD (DIS 2000)”, Liverpool, England, 2000, eds. J.A. Gracey and T. Greenshaw, World Scientific, 2001, p. 27.
- [18] S.G. Salesch, Ph.D. thesis, Hamburg University, 1993, DESY-93-196 (unpublished).
- [19] F. Aversa, P. Chiappetta, M. Greco, and J.-Ph. Guillet, Phys. Rev. Lett. **65**, 401 (1990); F. Aversa, P. Chiappetta, L. Gonzales, M. Greco, and J.-Ph. Guillet, Z. Phys. **C49**, 459 (1991).
- [20] J.-Ph. Guillet, Z. Phys. **C51**, 587 (1991).
- [21] S.B. Libby and G. Sterman, Phys. Rev. **D18**, 3252 (1978); R.K. Ellis, H. Georgi, M. Machacek, H.D. Politzer, and G.G. Ross, Phys. Lett. **78B**, 281 (1978); Nucl. Phys. **B152**, 285 (1979); D. Amati, R. Petronzio, and G. Veneziano, Nucl. Phys. **B140**, 54 (1980); Nucl. Phys. **B146**, 29 (1978); G. Curci, W. Furmanski, and R. Petronzio, Nucl. Phys. **B175**, 27 (1980); J.C. Collins, D.E. Soper, and G. Sterman, Phys. Lett. **B134**, 263 (1984); Nucl. Phys. **B261**, 104 (1985); J.C. Collins, Nucl. Phys. **B394**, 169 (1993).

- [22] L.E. Gordon and W. Vogelsang, Phys. Rev. **D50**, 1901 (1994).
- [23] N. Kidonakis, G. Oderda, and G. Sterman, Nucl. Phys. **B525**, 299 (1998).
- [24] J. Pumplin *et al.*, JHEP **0207**, 012 (2002).
- [25] M. Glück, E. Reya, M. Stratmann, and W. Vogelsang, Phys. Rev. **D63**, 094005 (2001).